

C 55.13: NESS 67

NOAA TR NESS 67

A UNITED STATES  
DEPARTMENT OF  
COMMERCE  
PUBLICATION



# NOAA Technical Report NESS 67

U.S. DEPARTMENT OF COMMERCE  
National Oceanic and Atmospheric Administration  
National Environmental Satellite Service

## Vertical Resolution of Temperature Profiles for High Resolution Infrared Radiation Sounder (HIRS)

Y. M. CHEN  
H. M. WOOLF  
W. L. SMITH

WASHINGTON, D.C.  
January 1974



## NOAA TECHNICAL REPORTS

### National Environmental Satellite Service Series

The National Environmental Satellite Service (NESS) is responsible for the establishment and operation of the National Operational Meteorological Satellite System and of the environmental satellite systems of NOAA. The three principal offices of NESS are Operations, Systems Engineering, and Research. The NOAA Technical Report NESS series is used by these offices to facilitate early distribution of research results, data handling procedures, systems analyses, and other information of interest to NOAA organizations.

Publication of a report in NOAA Technical Report NESS series will not preclude later publication in an expanded or modified form in scientific journals. NESS series of NOAA Technical Reports is a continuation of, and retains the consecutive numbering sequence of, the former series, ESSA Technical Report National Environmental Satellite Center (NESC), and of the earlier series, Weather Bureau Meteorological Satellite Laboratory (MSL) Report. Reports 1 through 37 are listed in publication NESC 56 of this series.

Reports 1 through 50 in the series are available from the National Technical Information Service (NTIS), U.S. Department of Commerce, Sills Bldg., 5285 Port Royal Road, Springfield, Va. 22151. Price \$3.00 paper copy; \$1.45 microfiche. Order by accession number, when given, in parentheses. Beginning with 51, printed copies of the reports are available through the Superintendent of Documents, U.S. Government Printing Office, Washington, D.C. 20402. Price as indicated. Microfiche available from NTIS (use accession number when available). Price \$1.45.

### ESSA Technical Reports

- NESC 38 Angular Distribution of Solar Radiation Reflected From Clouds as Determined From TIROS IV Radiometer Measurements. I. Ruff, R. Koffler, S. Fritz, J. S. Winston, and P. K. Rao, March 1967. (PB-174-729)
- NESC 39 Motions in the Upper Troposphere as Revealed by Satellite Observed Cirrus Formations. H. McClure Johnson, October 1966. (PB-173-996)
- NESC 40 Cloud Measurements Using Aircraft Time-Lapse Photography. Linwood F. Whitney, Jr., and E. Paul McClain, April 1967. (PB-174-728)
- NESC 41 The SINAP Problem: Present Status and Future Prospects; Proceedings of a Conference Held at the National Environmental Satellite Center, Suitland, Maryland, January 18-20, 1967. E. Paul McClain, October 1967. (PB-176-570)
- NESC 42 Operational Processing of Low Resolution Infrared (LRIR) Data From ESSA Satellites. Louis Rubin, February 1968. (PB-178-123)
- NESC 43 Atlas of World Maps of Long-Wave Radiation and Albedo--for Seasons and Months Based on Measurements From TIROS IV and TIROS VII. J. S. Winston and V. Ray Taylor, September 1967. (PB-176-569)
- NESC 44 Processing and Display Experiments Using Digitized ATS-1 Spin Scan Camera Data. M. B. Whitney, R. C. Doolittle, and B. Goddard, April 1968. (PB-178-424)
- NESC 45 The Nature of Intermediate-Scale Cloud Spirals. Linwood F. Whitney, Jr., and Leroy D. Herman, May 1968. (AD-673-681)
- NESC 46 Monthly and Seasonal Mean Global Charts of Brightness From ESSA 3 and ESSA 5 Digitized Pictures, February 1967-February 1968. V. Ray Taylor and Jay S. Winston, November 1968. (PB-180-717)
- NESC 47 A Polynomial Representation of Carbon Dioxide and Water Vapor Transmission. William L. Smith, February 1969. (PB-183-296)
- NESC 48 Statistical Estimation of the Atmosphere's Geopotential Height Distribution From Satellite Radiation Measurements. William L. Smith, February 1969. (PB-183-297)
- NESC 49 Synoptic/Dynamic Diagnosis of a Developing Low-Level Cyclone and Its Satellite-Viewed Cloud Patterns. Harold J. Brodrick and E. Paul McClain, May 1969. (PB-184-612)
- NESC 50 Estimating Maximum Wind Speed of Tropical Storms From High Resolution Infrared Data. L. F. Hubert, A. Timchalk, and S. Fritz, May 1969. (PB-184-611)

(Continued on inside back cover)



U.S. DEPARTMENT OF COMMERCE  
Frederick B. Dent, Secretary

NATIONAL OCEANIC AND ATMOSPHERIC ADMINISTRATION  
Robert M. White, Administrator

NATIONAL ENVIRONMENTAL SATELLITE SERVICE  
David S. Johnson, Director

## NOAA Technical Report NESS 67

# Vertical Resolution of Temperature Profiles for High Resolution Infrared Radiation Sounder (HIRS)

Y. M. Chen

H. M. Woolf

W. L. Smith



WASHINGTON, D.C.  
JANUARY 1974

For sale by the Superintendent of Documents, U.S. Government Printing Office, Washington, D.C., 20402.  
Price \$0.55

## CONTENTS

Abstract . . . . .	1
1. Introduction . . . . .	1
2. The Method of Backus and Gilbert . . . . .	1
3. Application to HIRS . . . . .	4
4. Discussion . . . . .	.12
Acknowledgements . . . . .	.12
References . . . . .	.14

Abstract

1. Introduction

2. The method of the present study

3. Application

4. Discussion

References

Appendix

# VERTICAL RESOLUTION OF TEMPERATURE PROFILES FOR HIGH RESOLUTION INFRARED RADIATION SOUNDER (HIRS)

Y. M. Chen\*, H. M. Woolf and W. L. Smith  
National Environmental Satellite Service  
National Oceanic and Atmospheric Administration  
Washington, D. C.

ABSTRACT. By using the method of Backus and Gilbert, the intrinsic vertical resolution of temperature profiles obtained from the High Resolution Infrared Radiation Sounder (HIRS) on the Nimbus-F satellite, which contains channels in both 4.3- $\mu$ m and 15- $\mu$ m CO<sub>2</sub> absorption bands, is evaluated and compared with those of channels in the 4.3- $\mu$ m band and the 15- $\mu$ m band alone. It is found that the combination of 4.3- $\mu$ m and 15- $\mu$ m bands is superior to the other two cases for all levels of the pressure.

## 1. INTRODUCTION

One of the basic problems in atmospheric temperature profile inversion techniques is the intrinsic vertical resolution of the measurement system. Recently, the fundamental technique for obtaining a direct quantitative value in answer to the problem was developed by Backus and Gilbert (1968, 1970) for the analysis of the solid earth. Conrath (1971) has applied it to the problem of the vertical sounding of the atmosphere by means of remote radiation measurements (with random noise) in the 15- $\mu$ m CO<sub>2</sub> absorption band.

The purposes of this paper are to evaluate the intrinsic vertical resolution of temperature profiles obtained from the High Resolution Infrared Sounder (HIRS) on the Nimbus-F satellite (which contains channels in both 4.3- $\mu$ m and 15- $\mu$ m CO<sub>2</sub> absorption bands) and to compare it with those obtained separately in the 4.3- $\mu$ m and 15- $\mu$ m bands. First, a brief review of the formulation of Backus and Gilbert is presented. Then for various levels of atmospheric pressure  $p$ , the averaging kernel  $A(x, x')$ , the center of  $A(x, x')$ , and the resolving length of  $A(x, x')$  are computed and plotted as functions of  $p$  for three individual cases, the 4.3- $\mu$ m band, the 15- $\mu$ m band and the 4.3- $\mu$ m + 15- $\mu$ m bands (HIRS). Finally, we discuss and compare these three cases.

## 2. THE METHOD OF BACKUS AND GILBERT

In the remote sensing of atmospheric temperature profiles, measurements are made of radiances in a finite number of spectral intervals within

---

\*Permanent address: Department of Applied Mathematics and Statistics  
State University of New York, Stony Brook, New York 11790

atmospheric absorption bands. For a nonscattering atmosphere in local thermodynamic equilibrium, the expression for the radiances has the form

$$I(v_i) = B[T(p_0), v_i] \tau(p_0, v_i) - \int_{x(0)}^{x(p_0)} B[T(p), v_i] \frac{d\tau(p, v_i)}{dx(p)} dx(p), \quad (1)$$

$$i = 1, 2, \dots, m,$$

where  $B[T(p), v]$  is the Planck function for temperature  $T(p)$  at pressure  $p$ ; the independent variable  $x$  can be any monotonic function of  $p$  ( $x = \ln p$  being used here);  $p_0$  is the surface pressure; and  $\tau(p, v_i)$  is the transmittance of the atmosphere above pressure  $p$  at  $v_i$ .

The inversion problem then is to estimate the temperature profile  $T(p)$ , given the atmospheric transmittances  $\tau(p, v_i)$  and measurements of the radiances  $\{I(v_i)\}$ ,  $i = 1, 2, \dots, m$ . If the contribution from the nonlinearity of eq (1) is small, then only the first iteration of the iterative algorithm of Chen (1973) or the procedure of Backus and Gilbert will be sufficient for our purpose. Hence, the contribution from nonlinearity is assumed to be small throughout.

Let

$$T(p) \approx T_0(p) + \delta T(p), \quad (2)$$

where  $T_0(p)$  is the reference profile and is taken to be the U.S. Standard Atmosphere. Then from Chen (1973),  $\delta T(p)$  should be the best approximate solution of the linearized equation

$$\int_{-\infty}^{x_0} K[x, v_i] \delta T(x) dx = \delta I(v_i), \quad i = 1, 2, \dots, m, \quad (3)$$

$$\text{where } K[x, v_i] \equiv \frac{d}{dx} \left[ \frac{B[T(x), v_i]}{T} \right] \bigg|_{T_0} \frac{d\tau(x, v_i)}{dx}, \quad (4)$$

$$\delta I(v_i) \equiv B[T_0(x_0), v_i] \tau(x_0, v_i) - \int_{-\infty}^{x_0} B[T_0(x), v_i] \frac{d\tau(x, v_i)}{dx} dx - I(v_i), \quad (5)$$

and  $dB/dT$  is the Fréchet derivative of  $B[T]$ .

The weighted average of  $\delta T$  at  $x$  which gives heavy emphasis to points close to  $x$  and very little to distant points is defined by

$$\langle \delta T \rangle_x = \int_{-\infty}^{x_0} A(x, x') \delta T(x') dx', \quad (6)$$

where the averaging kernel  $A$  is normalized according to



$$\int_{-\infty}^{x_0} A(x, x') dx' = 1. \quad (7)$$

$\langle \delta T \rangle_x$  is the most localized weighted average if and only if the averaging kernel  $A$  closely resembles the Dirac delta function  $\delta(x'-x)$ . The spread of  $A$  from  $x$  is defined by

$$Q(x, A) \equiv \alpha_J \int_{-\infty}^{x_0} J(x, x') A^2(x, x') dx', \quad (8)$$

where  $J(x, x')$  is a chosen infinitely differentiable function of  $x'$  such that  $J(x, x) = 0$  and increases monotonically as  $x'$  increases or decreases away from  $x$  with dimension of  $x'^2$ , and

$$\alpha_J \equiv \frac{\ell}{\int_{-\infty}^{x_0} J(x, x') A_\ell^2(x, x') dx'} \quad (9)$$

$$\text{with } A_\ell(x, x') \equiv 1/\ell, \quad x - \ell/2 < x' < x + \ell/2, \quad \left\{ \begin{array}{l} 0, \quad |x' - x| \geq \ell/2, \end{array} \right. \quad (10)$$

$$\text{Note that } Q(x, A_\ell) = \ell \quad (\text{the spread of } A_\ell). \quad (11)$$

If  $A$  has a sharp peak, the choice of  $J$  is rather free. However, if  $A$  has a blurred peak, the selection of  $J$  is much more critical. Throughout,

$$J(x, x') = (x - x')^2 \quad (12)$$

is used. ( $\alpha_J = 12$ .) As one will see later, this choice of  $J$  is not very good for 4.3- $\mu\text{m}$   $\text{CO}_2$  channels in the upper stratosphere ( $p \approx 8 - 60$  mb).

Equation (3) shows that  $\{\delta I(v_i)\}$ ,  $i = 1, 2, \dots, m$ , are  $m$  bounded linear functionals of  $\delta T(x)$ . Since  $\langle \delta T \rangle_x$  and  $\{\delta I(v_i)\}$ ,  $i = 1, 2, \dots, m$ , all depend linearly on the function  $\delta T$ , it follows that  $\langle \delta T \rangle_x$  must depend linearly on  $\{\delta I(v_i)\}$ . Therefore, there should exist constants  $\{a_i(x)\}$ ,  $i = 1, 2, \dots, m$ , depending on the fixed point  $x$  such that

$$\langle \delta T \rangle_x = \sum_{i=1}^m a_i(x) \delta I(v_i). \quad (13)$$

Hence from (3) and (6),

$$A(x, x') = \sum_{i=1}^m a_i(x) K[x', v_i]. \quad (14)$$

It follows from (8) and (14) that  $Q(x, A)$  is a positive-definite quadratic function of  $\{a_i(x)\}$ . Since the determination of the most localized weighted

average  $\langle \delta T \rangle_x$  is equivalent to minimizing the spread of  $A$  from  $x$ , subject to the constraint (7), by using the method of Lagrange multipliers, the proper set of  $\{a_i(x)\}$  satisfies the following set of  $m+1$  linear algebraic equations:

$$\left. \begin{aligned} \sum_{j=1}^m \left\{ 12 \int_{-\infty}^{x_0} (x-x')^2 K[x', v_i] K[x', v_j] dx' \right\} a_j(x) + \lambda \int_{-\infty}^{x_0} K[x', v_i] dx' &= 0, \\ i &= 1, 2, \dots, m, \\ \sum_{j=1}^m \left\{ \int_{-\infty}^{x_0} K[x', v_j] dx' \right\} a_j(x) &= 1, \end{aligned} \right\} \quad (15)$$

where  $\lambda$  is a Lagrange multiplier.

The vertical resolution of the temperature profile at the level  $x$  obtainable from a given set of radiance measurements is determined by the closeness of  $A(x, x')$  to  $\delta(x' - x)$ . Visually, the plot of  $A(x, x')$  vs.  $x'$  gives a qualitative estimate of the vertical resolution at  $x$ . To characterize the behavior of  $A(x, x')$  more precisely, the "resolving length" of  $A(x, x')$  is introduced and defined as the spread about its center,

$$w(x) = 12 \int_{-\infty}^{x_0} [c(x) - x']^2 A^2(x, x') dx', \quad (16)$$

where

$$c(x) = \int_{-\infty}^{x_0} x' A^2(x, x') dx' / \int_{-\infty}^{x_0} A^2(x, x') dx' \quad (17)$$

is the "center" of  $A(x, x')$ .

### 3. APPLICATION TO, HIRS

The method of Backus and Gilbert has been applied to an analysis of the vertical resolution of temperature profiles inferred from radiance measurements in two  $\text{CO}_2$  absorption bands observed by the High Resolution Infrared Radiation Sounder (HIRS). The 7 channels in the  $15\text{-}\mu\text{m}$   $\text{CO}_2$  band and the 5 channels in the  $4.3\text{-}\mu\text{m}$   $\text{CO}_2$  band in the study are listed in table 1. The  $d\tau_i/dx(p)$  vs.  $p$  curves for  $15\text{-}\mu\text{m}$  and  $4.3\text{-}\mu\text{m}$   $\text{CO}_2$  bands are shown in figures 1 and 2 respectively. Similarly, the  $dB_i/dT|_{T_0} \cdot d\tau_i/dx(p)$  radiative transfer kernels vs.  $p$  for  $15\text{-}\mu\text{m}$  and  $4.3\text{-}\mu\text{m}$   $\text{CO}_2$  bands are shown in figure 3. The averaging kernel  $A$  for each of various pressure levels, ranging from 1 mb to 1000 mb, is computed for 3 separate cases: the 5 channels in the  $4.3\text{-}\mu\text{m}$  band alone, the 7 channels in the  $15\text{-}\mu\text{m}$  band alone, and the 12 channels in the combination of  $4.3\text{-}\mu\text{m}$  and  $15\text{-}\mu\text{m}$  bands. The corresponding set of three averaging kernels at various levels of  $p$  are plotted as functions of atmospheric pressure in figures 4 to 12. These curves give a qualitative estimate of the vertical resolution at the indicated levels and offer a visual comparison for the resolving length and the center of  $A(x, x')$  among the

Table 1.--HIRS channel spectral characteristics

CO <sub>2</sub> band	Channel no.	Center frequency (cm <sup>-1</sup> )
15 μm	1	668.5
	2	680.0
	3	690.0
	4	703.0
	5	716.0
	6	733.0
	7	749.0
4.3 μm	11	2190.0
	12	2210.0
	13	2240.0
	14	2270.0
	15	2360.0

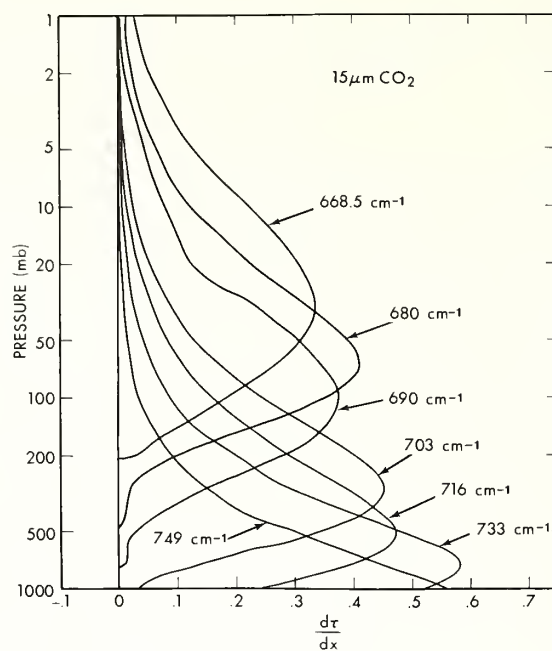


Figure 1.--The derivative of transmittance with respect to the logarithm of pressure for the 15- $\mu\text{m}$   $\text{CO}_2$  absorption band.

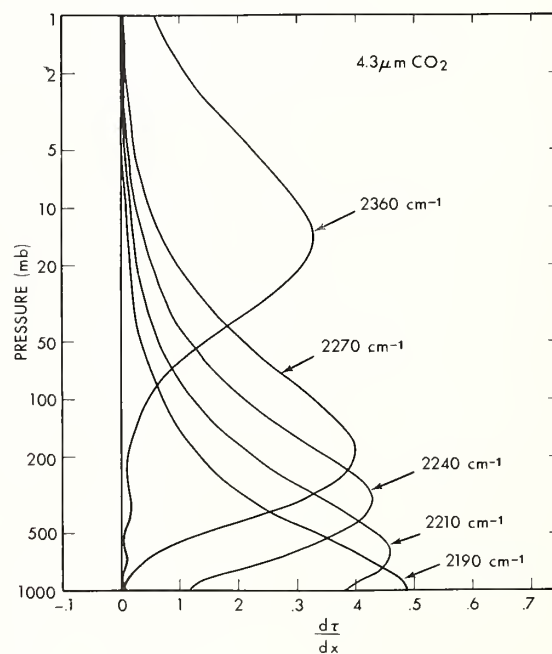


Figure 2.--The derivative of transmittance with respect to the logarithm of pressure for the 4.3- $\mu\text{m}$   $\text{CO}_2$  absorption band.

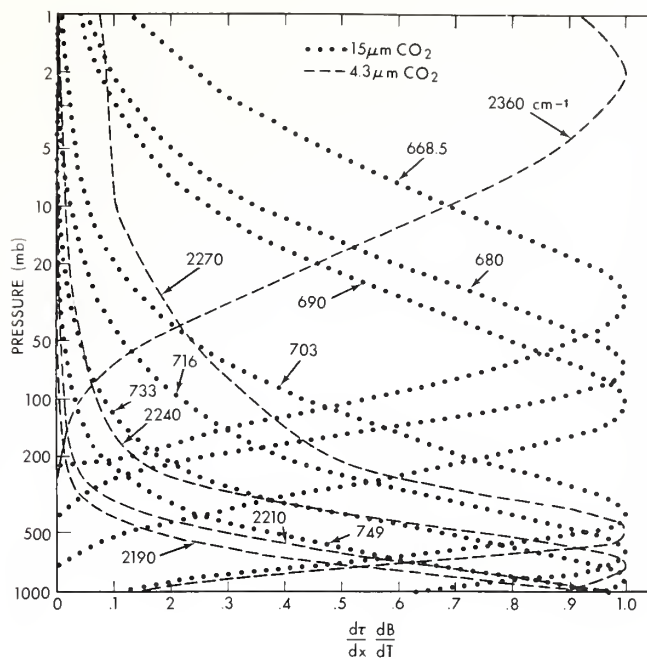


Figure 3.--Radiative transfer kernels for the 15- $\mu\text{m}$  and 4.3- $\mu\text{m}$   $\text{CO}_2$  absorption bands vs. pressure.

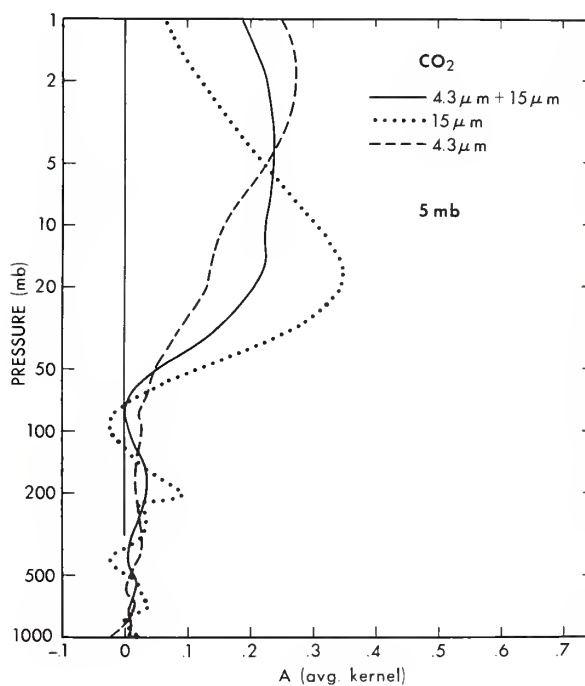


Figure 4.--Averaging kernels at 5 mb for the 4.3- $\mu\text{m}$  band, 15- $\mu\text{m}$  band and 4.3- $\mu\text{m}$  + 15- $\mu\text{m}$  bands plotted as functions of atmospheric pressure.

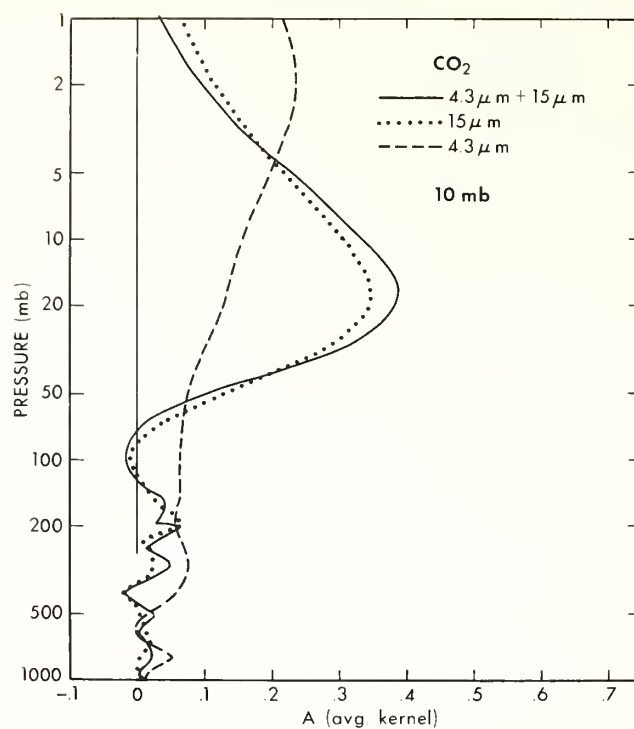


Figure 5.--Averaging kernels at 10 mb for the 4.3- $\mu$ m band, 15- $\mu$ m band, and 4.3- $\mu$ m + 15- $\mu$ m bands plotted as functions of atmospheric pressure.

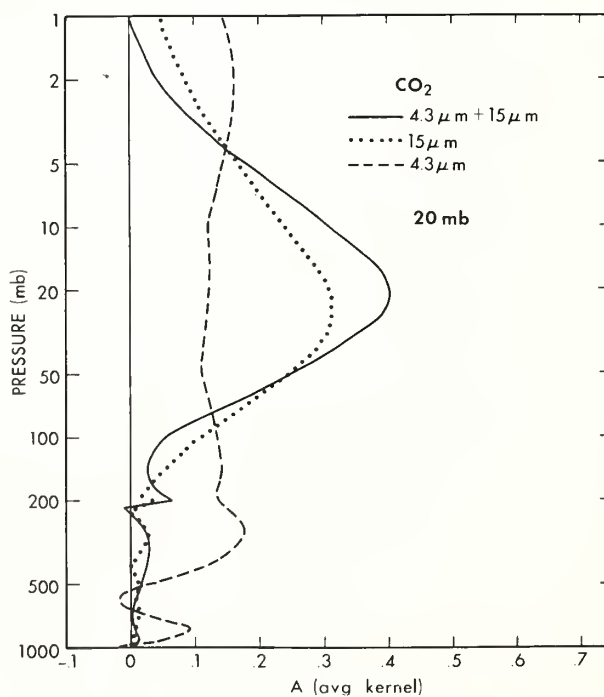


Figure 6.--Averaging kernels at 20 mb for the 4.3- $\mu$ m band, 15- $\mu$ m band, and 4.3- $\mu$ m + 15- $\mu$ m bands plotted as functions of atmospheric pressure.

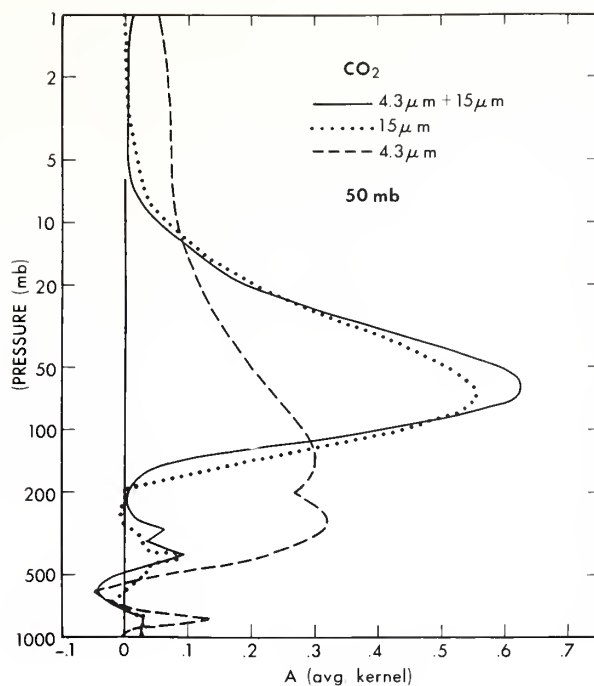


Figure 7.--Averaging kernels at 50 mb for the 4.3- $\mu$ m band, 15- $\mu$ m band, and 4.3- $\mu$ m + 15- $\mu$ m bands plotted as functions of atmospheric pressure.

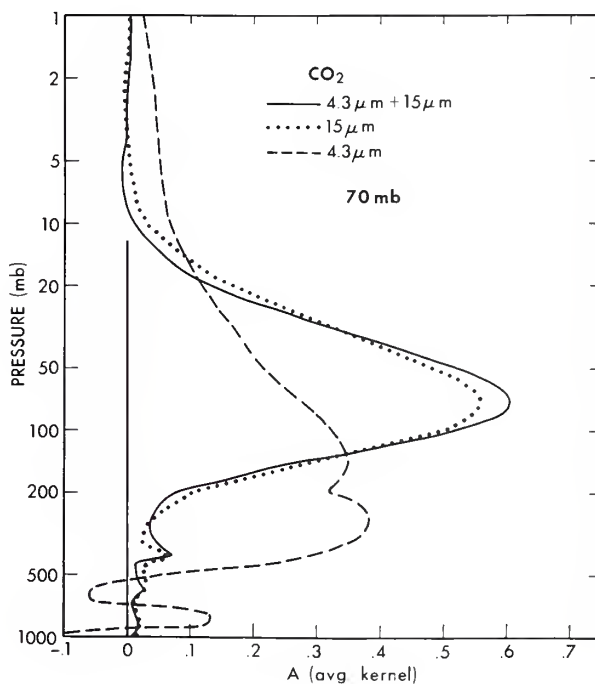


Figure 8.--Averaging kernels at 70 mb for the 4.3- $\mu$ m band, 15- $\mu$ m band, and 4.3- $\mu$ m + 15- $\mu$ m bands plotted as functions of atmospheric pressure.

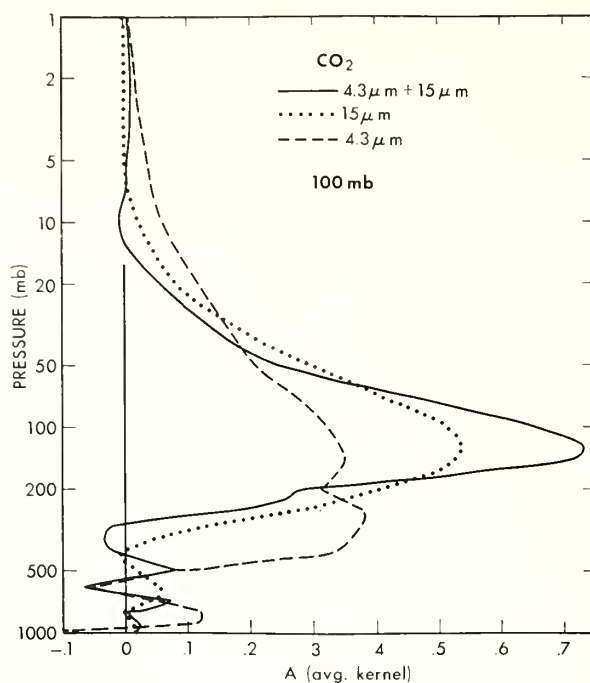


Figure 9.--Averaging kernels at 100 mb for the 4.3- $\mu$ m band, 15- $\mu$ m band, and 4.3- $\mu$ m + 15- $\mu$ m bands plotted as functions of atmospheric pressure.

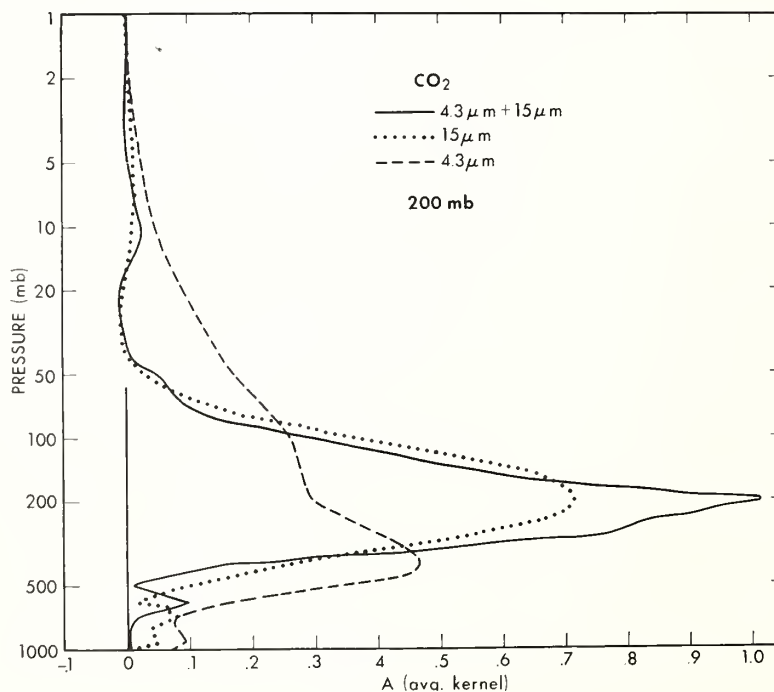


Figure 10.--Averaging kernels at 200 mb for the 4.3- $\mu$ m band, 15- $\mu$ m band, and 4.3- $\mu$ m + 15- $\mu$ m bands plotted as functions of atmospheric pressure.



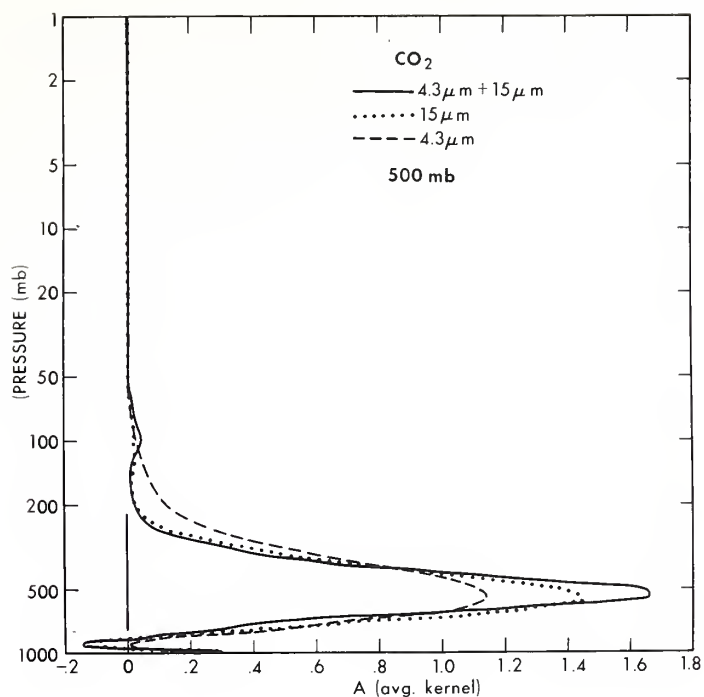


Figure 11.--Averaging kernels at 500 mb for the 4.3- $\mu$ m band, 15- $\mu$ m band, and 4.3- $\mu$ m + 15- $\mu$ m bands plotted as functions of atmospheric pressure.

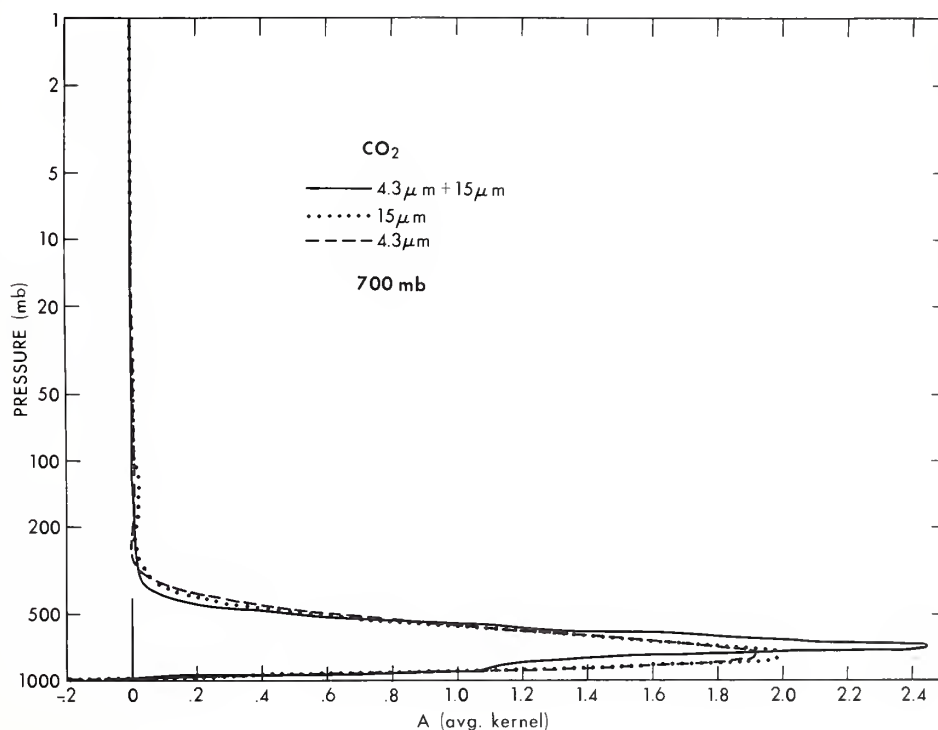


Figure 12.--Averaging kernels at 700 mb for the 4.3- $\mu$ m band, 15- $\mu$ m band, and 4.3- $\mu$ m + 15- $\mu$ m bands plotted as functions of atmospheric pressure.

three cases. Finally, the center and the resolving of  $A(x, x')$  for the above-mentioned three cases are computed and plotted in figures 13 and 14, respectively.

#### 4. DISCUSSION

Qualitatively, the curves of figures 4 to 12 indicate that the 12 channels of the combined 4.3- $\mu\text{m}$  and 15- $\mu\text{m}$   $\text{CO}_2$  bands has better vertical resolution of temperature profiles than that of the 7 channels of the 15- $\mu\text{m}$  band, uniformly for all  $p$ , which in turn has better vertical resolution than that of the 5 channels of the 4.3- $\mu\text{m}$  band. This is substantiated by the center vs.  $p$  curves in figure 13 and the resolving length  $w(p)$  vs.  $p$  curves in figure 14. It is found that the addition of the 5 channels of the 4.3- $\mu\text{m}$  band to the 15- $\mu\text{m}$  band improves the resolving length of the averaging kernel for the 15- $\mu\text{m}$  band alone about 1 to 15% in the troposphere, 15 to 43% in the stratosphere except in the range of 3.5 to 8.5 mb, and 15% at the tropopause. Note that the  $w(p)$  vs.  $p$  curve for the 15- $\mu\text{m}$  band is comparable to that of Conrath (1971). Furthermore, figure 13 shows that in general the center of the averaging kernel for the combination of 4.3- $\mu\text{m}$  and 15- $\mu\text{m}$  bands is closer to the level to which the kernel pertained than the other two cases. This is particularly true in the upper stratosphere, for example in the layer of  $p < 10$  mb. Although the resolving length of the 15- $\mu\text{m}$  band is shorter than that of the combined 4.3- $\mu\text{m}$  and 15- $\mu\text{m}$  bands in the range of 3.5 to 8.5 mb, the large deviation of the center of the averaging kernel for the 15- $\mu\text{m}$  band from the level to which the kernel pertains does away with any advantage of shorter resolving length. In our opinion, these facts indicate the uniform superiority of the combination of 4.3- $\mu\text{m}$  and 15- $\mu\text{m}$  bands over the other two cases for all  $p$  in the vertical resolution of temperature profiles.

Figure 14 indicates that the resolving length for the 4.3- $\mu\text{m}$   $\text{CO}_2$  channels is poor in the range of 8 to 60 mb. This is mainly because of the lack of weight concentration of  $K[x, v_i]$ 's in that particular range (figure 4). Unfortunately, the method of Backus and Gilbert will not yield accurate results under this circumstance. To obtain more accurate results, one has to experiment with various  $J$ -functions other than that of eq (12).

It is known that the instrument noise will contaminate the above results (Backus and Gilbert, 1970). The general effect of the noise here is believed to be the same as that in the analysis of Conrath (1971).

#### ACKNOWLEDGEMENTS

The authors wish to thank Messrs. C. M. Jacobson, L. P. Mannello and L. D. Hatton for their assistance in the preparation of this paper. One of the authors (YMC) also wishes to express his appreciation to Dr. J. S. Winston for a very pleasant stay (summer, 1972) at the Meteorological Satellite Laboratory, National Environmental Satellite Service, NOAA, where this research was carried out.

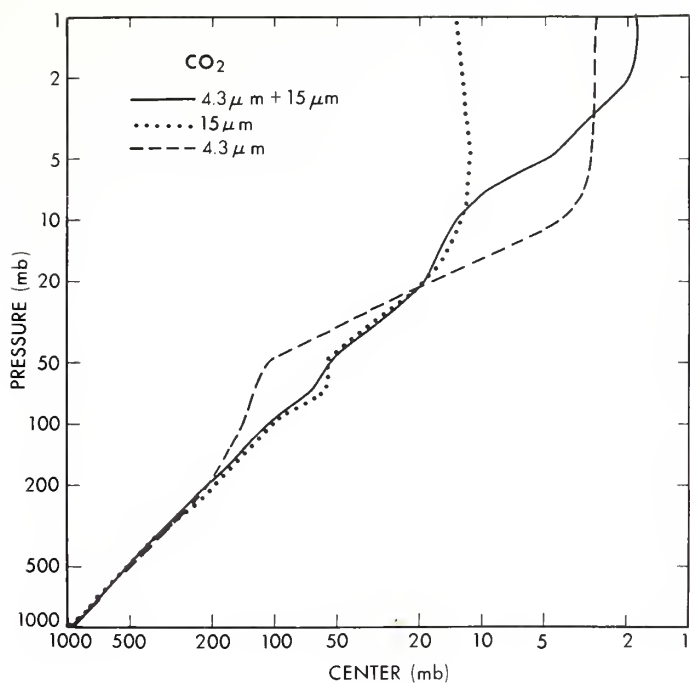


Figure 13.--Averaging kernel center for the 4.3- $\mu$ m band, 15- $\mu$ m band, and 4.3- $\mu$ m + 15- $\mu$ m bands plotted as functions of atmospheric pressure.

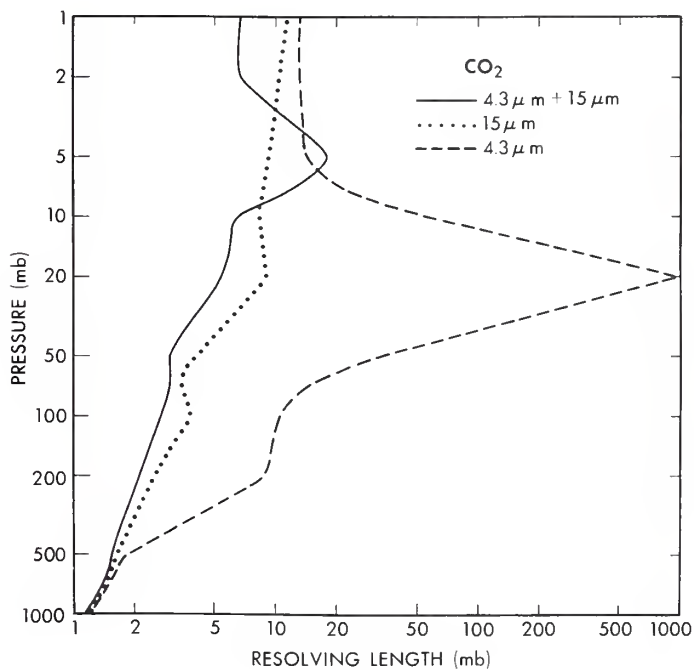


Figure 14.--Resolving lengths for the 4.3- $\mu$ m band, 15- $\mu$ m band, and 4.3- $\mu$ m + 15- $\mu$ m bands plotted as functions of atmospheric pressure.

## REFERENCES

- Backus, George, E. and Gilbert, J. Freeman, "The Resolving Power of Gross Earth Data," Geophysics Journal Royal Astronomical Society, Vol. 16, pp. 169-205, 1968.
- Backus, George, E. and Gilbert, J. Freeman, "Uniqueness in the Inversion of Inaccurate Gross Earth Data," Philosophical Transactions Royal Society of London, Vol. A266, pp. 123-192, 1970.
- Chen, Yung Ming, "Iterative Algorithms for Constructing Approximate Solutions of Nonlinear Problems from Inadequate Data," Unpublished Manuscript, 1973.
- Conrath, Barney J., "Vertical Resolution of Temperature Profiles Obtained from Remote Radiation Measurements," NASA (Goddard Space Flight Center) preprint X-622-71-519, 1971.





- NESC 51 Application of Meteorological Satellite Data in Analysis and Forecasting. Ralph K. Anderson, Jerome P. Ashman, Fred Bittner, Golden R. Farr, Edward W. Ferguson, Vincent J. Oliver, and Arthur H. Smith, September 1969. Price \$1.75 (AD-697-033) Supplement price \$0.65 (AD-740-Q17)
- NESC 52 Data Reduction Processes for Spinning Flat-Plate Satellite-Borne Radiometers. Torrence H. MacDonald, July 1970. Price \$0.50 (COM-71-00132)
- NESC 53 Archiving and Climatological Applications of Meteorological Satellite Data. John A. Leese, Arthur L. Booth, and Frederick A. Godshall, July 1970. Price \$1.25 (COM-71-00076)
- NESC 54 Estimating Cloud Amount and Height From Satellite Infrared Radiation Data. P. Krishna Rao, July 1970. Price \$0.25 (PB-194-685)
- NESC 56 Time-Longitude Sections of Tropical Cloudiness (December 1966-November 1967). J. M. Wallace, July 1970. Price \$0.50 (COM-71-00131)

NOAA Technical Reports

- NESS 55 The Use of Satellite-Observed Cloud Patterns in Northern Hemisphere 500-mb Numerical Analysis. Roland E. Nagle and Christopher M. Hayden, April 1971. Price \$0.55 (COM-73-50262)
- NESS 57 Table of Scattering Function of Infrared Radiation for Water Clouds. Giichi Yamamoto, Masayuki Tanaka, and Shoji Asano, April 1971. Price \$1.00 (COM-71-50312)
- NESS 58 The Airborne ITPR Brassboard Experiment. W. L. Smith, D. T. Hilleary, E. C. Baldwin, W. Jacob, H. Jacobowitz, G. Nelson, S. Soules, and D. Q. Wark, March 1972. Price \$1.25 (COM-72-10557)
- NESS 59 Temperature Sounding From Satellites. S. Fritz, D. Q. Wark, H. E. Fleming, W. L. Smith, H. Jacobowitz, D. T. Hilleary, and J. C. Alishouse, July 1972. Price \$0.55 (COM-72-50963)
- NESS 60 Satellite Measurements of Aerosol Backscattered Radiation From the Nimbus F Earth Radiation Experiment. H. Jacobowitz, W. L. Smith, and A. J. Drummond, August 1972. Price \$0.25 (COM-72-51031)
- NESS 61 The Measurement of Atmospheric Transmittance From Sun and Sky With an Infrared Vertical Sounder. W. L. Smith and H. B. Howell, September 1972. Price \$0.30 (COM-73-50020)
- NESS 62 Proposed Calibration Target for the Visible Channel of a Satellite Radiometer. K. L. Coulson and H. Jacobowitz, October 1972. Price \$0.35 (COM-73-10143)
- NESS 63 Verification of Operational SIRS B Temperature Retrievals. Harold J. Brodrick and Christopher M. Hayden, December 1972. Price \$0.55 (COM-73-50279)
- NESS 64 Radiometric Techniques for Observing the Atmosphere From Aircraft. William L. Smith and Warren J. Jacob. January 1973. Price \$0.35 (COM-73-50376)
- NESS 65 Satellite Infrared Soundings From NOAA Spacecraft. L. M. McMillin, D. Q. Wark, J.M. Siomkajlo, P. G. Abel, A. Werbowetzki, L. A. Lauritson, J. A. Pritchard, D. S. Crosby, H. M. Woolf, R. C. Luebke, M. P. Weinreb, H. E. Fleming, F. E. Bittner, and C. M. Hayden, September 1973. (COM-73-50936/6AS)
- NESS 66 Effects of Aerosols on the Determination of the Temperature of the Earth's Surface From Radiance Measurements at 11.2  $\mu\text{m}$ . H. Jacobowitz and K. L. Coulson, September 1973.

PENN STATE UNIVERSITY LIBRARIES



A000072018378